

Effect of electrodes' dissimilar and similar diameters on the microstructural and mechanical properties of resistance spot welds

Hamza ESSOUSSI¹, Said ETTAQI¹

¹Laboratory of Materials, Metallurgy and Process Engineering, ENSAM, Meknes, Morocco

Corresponding Author:hamza.essoussi1@gmail.com

Abstract: This paper deals with the study of steel sheet welds using the resistance spot welding technique with similar and dissimilar electrode diameters. Microstructural and mechanical properties of the performed welds were investigated using respectively optical microscope, shear and cross tensile tests, as well as micro-hardness measurements. The results revealed that the strength of welds increased with the increase of dissimilarity of electrodes' diameters. the size and the form of the obtained nuggets vary strongly with the electrode diameter.

Keywords: Resistance spot welding(RSW); Nugget size; Nugget shape; Micro-hardness; Weldability

Date of Submission: 11-12-2020

Date of Acceptance: 26-12-2020

I. INTRODUCTION

Resistance spot welding RSW process was primarily developed and known as a potential welding process used in the automotive industry owing to nowadays several thousand spot-welded joints are present in cars. Consequently, numerous studies have been conducted to allow a better understanding of the possible parameters that can affect the performance of the realized spot welds[1]–[3]. Generally, the weldability of steels using the RSW process depends strongly on the steels' chemical composition [4]. Thus, higher amounts of carbon and other alloying elements results in a higher hardenability and thus lower weldability. While, with lower additions of alloying elements, the resultant microstructure is mostly bainitic. While in the case of steels characterized by high alloying elements RSW welding gives rise to the martensitic phase in the nugget[5].

Earlier works have divided the welding parameters into intrinsic that depend on the materials to join such sheet thickness and chemical composition, while the extrinsic parameters are related to the applied electric current, pressure, time electrode properties such dimension, shape, and material. Particularly, the shape of used electrode in RSW process has been found to play a major role in affecting the weldability. Although, it is well reported that steels can be welded with all electrodes shape [6]. There are six standard faces designs of electrodes, the pointed nose electrodes are found to be a good general-purpose weld face suitable for most spot welding applications, while dome-shaped electrode tips (Type E, G & F) have been found capable to provide more consistent welds than truncated cone-shaped tips (Type A & B) [7].

On the other hand, the increased contact area leads to reduced current density. As a result, electrodes increase the current required to produce a large weld. Indeed, the flat-shaped electrode type “C” is frequently used as a back up electrode for projection welding. As well, it also is used for heat balancing. The use of the “C” face on one side of the weld reduces the indentation by spreading the force and current on that side over a larger area. In the case of heat balancing the “C” flat face is used to spread the current out over a large surface area[7–9].

After mechanical testing, three types of weld failure mode are commonly defined to classify weld failure of RSW joints, then to give a qualitative assessment of the material weldability: (i) full plug failure, (ii) partial plug failure, and (iii) interfacial failure. Indeed, Mahmoud et al reported that large spot welds submitted

to shear loads were shown to fail by strain localization in the base metal (BM) close to the weld, and smaller ones would fail at the faying surface with sheared fracture surfaces [1].

The present paper aims to highlight the microstructural and mechanical properties and failure mode analysis of the welds obtained using flat type electrodes with both similar and dissimilar electrodes diameter, through an optical microscope, micro-hardness measurements, as well as a cross, and shear tensile tests.

II. EXPERIMENTAL PROCEDURE

The material selected in the study is the 1000 Serie steel grade with the following chemical composition determined using an X-ray fluorescence spectrometer 0.01C-0.24Mn-Cu-0.02Cu-0.06V-99.67Fe (wt.%). the used steel was chosen for its good weldability. First, all samples were ultrasonically degreased using ultrasonic cleaner before the welding step to maintain consistent and clean surface conditions. Cross-sectional profiles of electrodes' similar and dissimilar diameters used for welding tests in this study are schematically illustrated in Fig.1, which presents the RSW process and dimensions of the electrodes used. Therefore, only the electrodes' diameters were varied, while the other welding conditions were fixed for all samples. Consequently, depending the electrode's diameter three tests were conducted (d_8/d_8), (d_8/d_6) and (d_8/d_4).

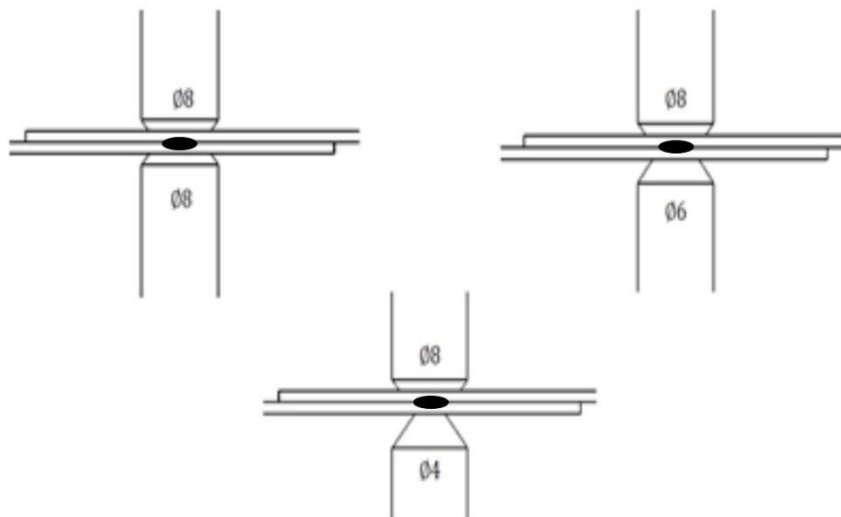


Figure 1: Schematic illustration of the welds performed in this study

For metallographic preparation, the welds obtained from each condition were sectioned through the weld center perpendicular to the plane of weld surface and then mounted, polished, and etched with Nital 4%. The observation of the cross-section of spot welds resulted from both mechanical tests were conducted using Olympus optical microscope (OM). Vickers-type microhardness measurements were performed under conditions of 100gf as load and a dwell time of 10s using a digital micro-hardness tester, the minimum distance between the centers of adjacent indentations should be at least 2.5times the diagonal of the expected minimum hardness (the lowest hardness indent will have the largest indent size), to avoid interactions between their regions of influence as specified in the ASTM E384-11 standard. On the other hand, to highlight the welds' mechanical properties, the welded samples were then submitted to complete cross tension and tensile shear tests at a speed of 2mm/min. and three aspects are compared (i) cross tensile force, (ii) shear tensile force, and (iii) failure mode after each mechanical test type.

III. RESULTS AND DISCUSSIONS

3.1 Microstructural properties

It is commonly accepted that the microstructural and mechanical properties of welds resulted from the process of resistance spot welding depend strongly on the chemical composition of the base metal. Thus, three regions can be identified: the weld nugget, the heat-affected zone (HAZ), and the unaffected base material. Fig. 2 shows the micrographs of the cross section of welds resulted from electrodes with similar and dissimilar

diameters d8/d8, d8/d6, and d8/d4. These optical micrographs of the performed welds depict a difference in nugget shape, size as well as in grain size as we move from the base metal (BM) to the heat-affected zone (HAZ) to the fusion zone (FZ).

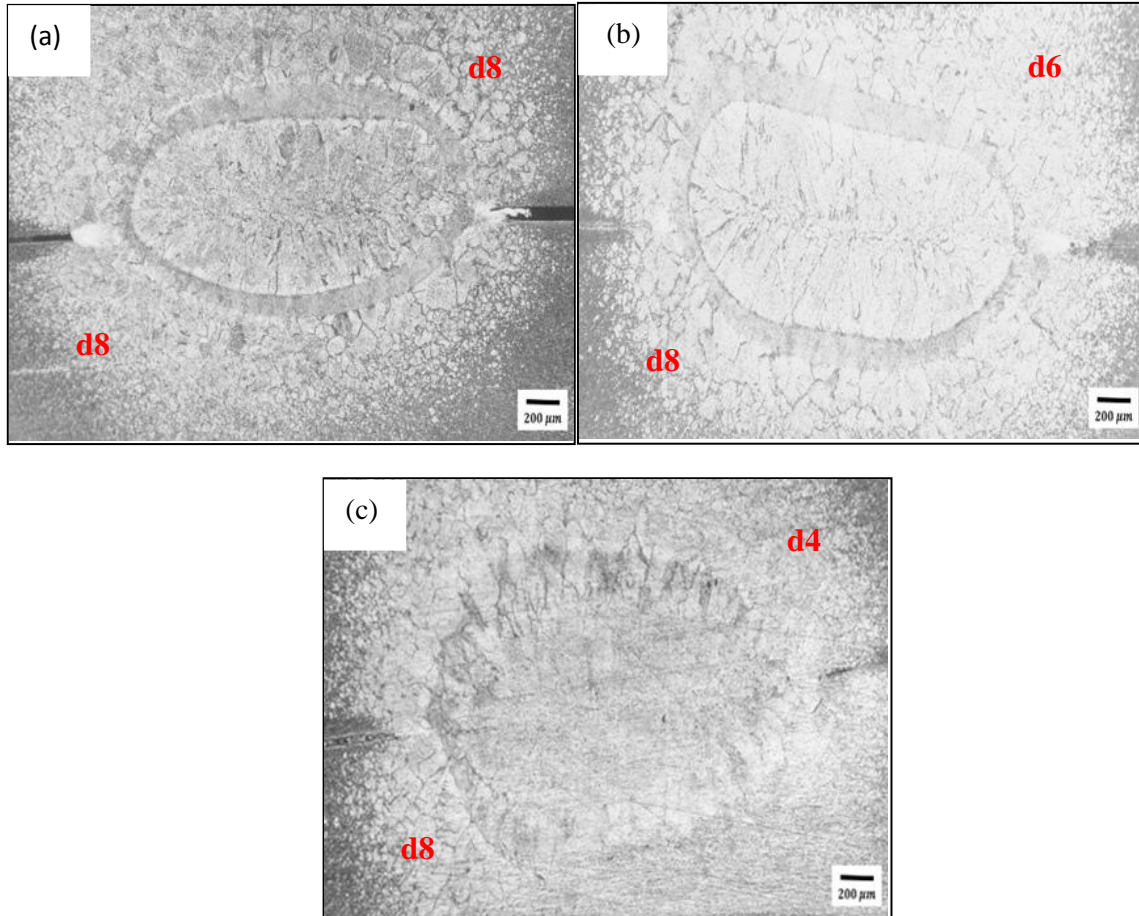


Figure 2: Optical micrographs showing the fusion zone (FZ), heat-affected zone (HAZ), and base metal (BM) of (a) (d8/d8) ; (b) : (d8/d6) and (c) : (d8/d4)

Depending on the flat-type electrodes diameters, different heat transfer may be generated. Thus, the nugget's size and shape vary from sample to another. While, in our case, due low carbon and other alloying elements percentage of the used steel, the nugget microstructure of all samples shows the presence of bainitic phase characterized by coarse grains elongated vertically along the cooling occurred after separating electrodes at the end of welding step, and horizontally along the centre line where cooling is directed to the surrounding material, such result was reported by Chan et al [7].

Moreover different HAZ (Heat Affected Zone) are observed. In the case of samples welded with similar diameters of electrodes (d8/d8), a narrow HAZ (due to the low thermal conductivity induced by large contact surface and high heat dissipation during RSW process) and softening (due to grain growth) are observed. However, large HAZ is seen in the case of samples welded with dissimilar diameter of electrodes, especially the larger one is that obtained using electrodes with significant dissimilarity of diameters $d=8\text{mm}$ and $d=4\text{mm}$.

3.2 Microhardness measurement

In this section macrographs and microhardness distribution across the welded structure of all performed welds are compared.

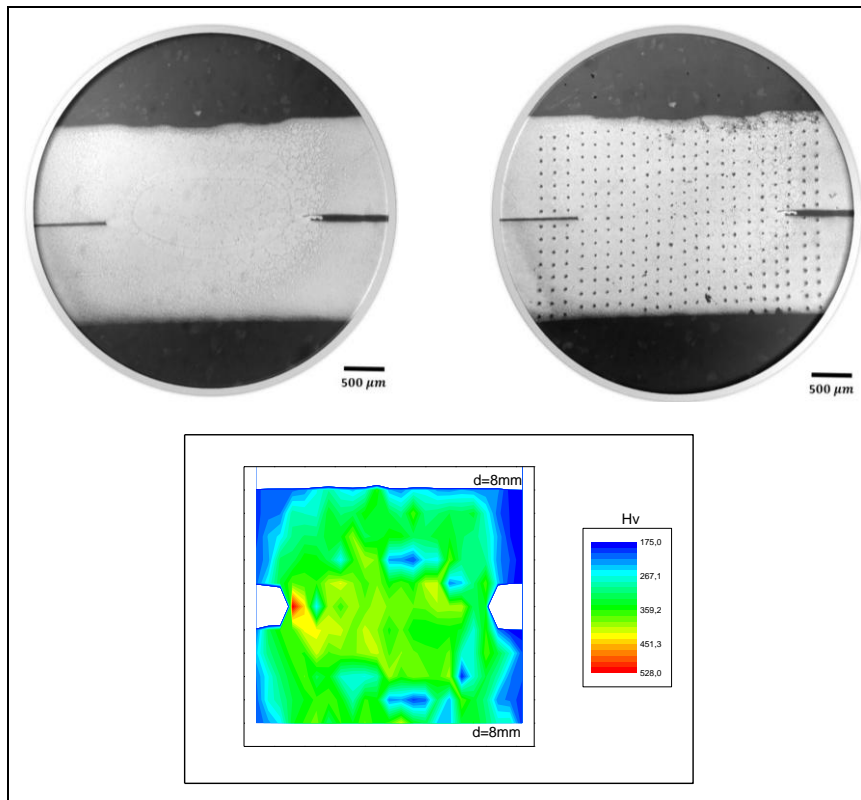


Figure 3: Longitudinal-sectional view of the performed weld and Microhardness distribution mapping of the weld obtained using electrodes with dissimilar diameters d8/d8

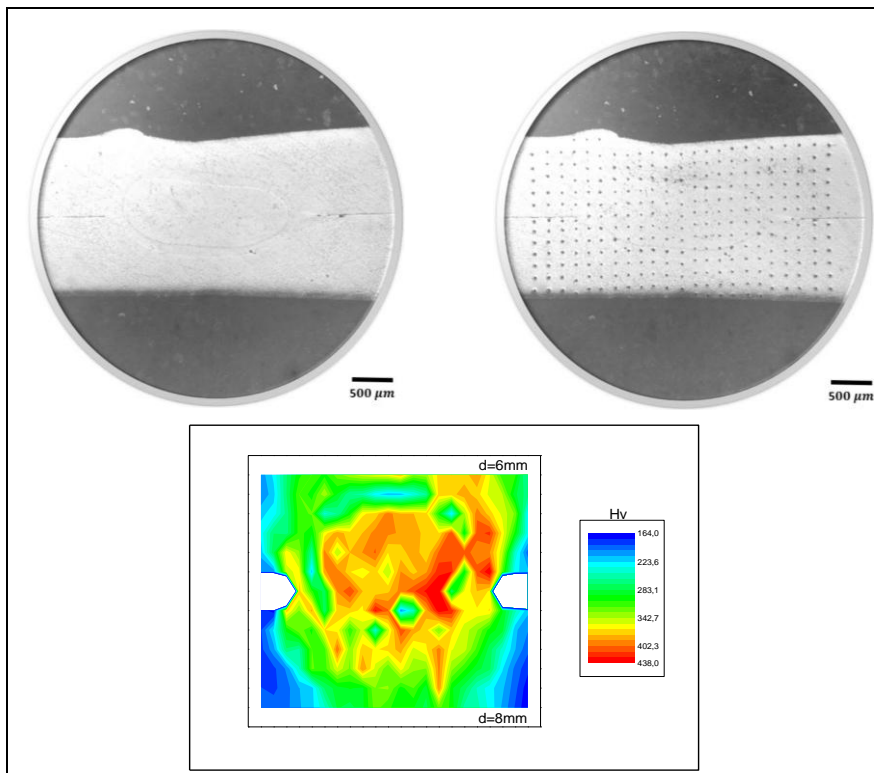


Figure 4: Longitudinal-sectional view of the performed weld and Microhardness distribution mapping of the weld obtained using electrodes with dissimilar diameters d8/d6

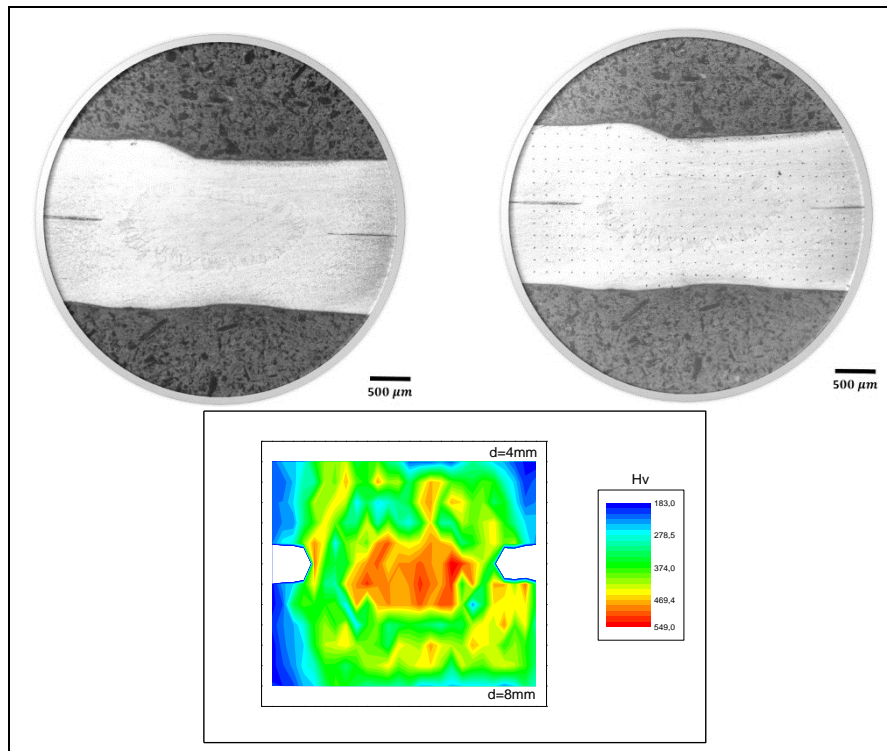


Figure 5: Longitudinal-sectional view of the performed weld and Microhardness distribution mapping of the weld obtained using electrodes with dissimilar diameters d_8/d_4

Fig. 3, Fig.4 and Fig.5 show respectively the macrographs and vickers microhardness distribution mapping of all performed welds using electrodes with similar (d_8/d_8) and dissimilar ((d_8/d_6) , (d_8/d_4)) diameters. Indeed, a clear dependence of the microhardness distribution with the electrode's diameter used for the welding operations is observed. First, for the specimen welded using flat electrodes with similar diameters (d_8/d_8) microhardness mapping shows homogeneous distribution, as well as the microhardness of the nugget region varies between 350 Hv and 450Hv, while the higher value 528Hv is measured outside the HAZ near to the unwelded region. Moreover, the lower hardness value were measured in the base metal and are about 175Hv. For the specimen welded using the same electrodes type with diameters equal respectively to 8mm and 6mm the higher hardness value (430Hv) is found at the nugget region, and outside the HAZ in the side of electrode with 4mm diameter, while its opposite side shows low values 180-230 Hv comparable to that obtained in the base metal. finally, the third sample welded using electrodes' diameters 8mm and 4mm the Hv mapping distribution shows heterogeneous distribution with high Hv of roughly 545 Hv at the middle of the nugget, outside the HAZ and homogeneous distribution is seen and the average hardness varies between 280 and 370 Hv, the metal base hardness in this case exhibited a value of 180Hv. Therefore the higher microhardness values measured are mainly due to the grain refinement.

3.3 Cross tensile behavior

Mechanical properties are determined through different tests to reveal important welds characteristics such as the maximum force measured during testing and weld failure mode. First, the so-called cross tensile tests of all welds obtained using electrodes with both similar and dissimilar diameters are presented in Fig.6.

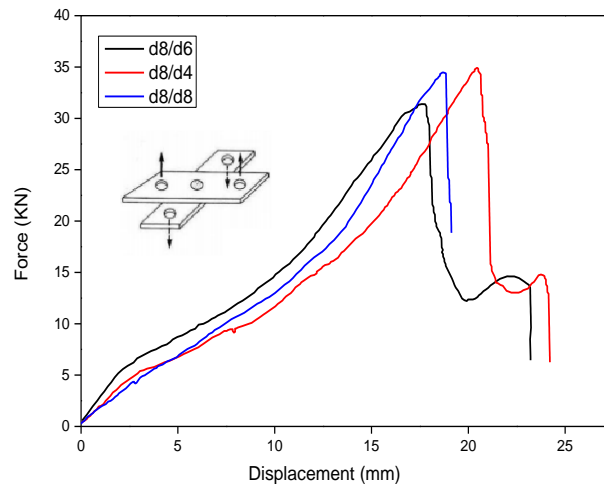


Figure 6: Cross-tensile curves of all performed welds: d8/d8, d8/d6, d8/d4

From Fig.6, it can be seen that the peak strength increased with the decrease of the diameter of the electrode used for welding. Indeed, the high strength was found in the samples welded using electrodes with dissimilar diameters especially diameters 8mm and 4mm, this is because during the welding process, lower diameter increased the heat transfer due to high current density compared to that generated by the electrodes with higher diameter, such a result was confirmed by the microstructural results that revealed uniform and bigger nuggets than those obtained under the other conditions. On the other hand, the qualitative analysis of weld's failure mode quality provides an extra information concerning whether fracture is brittle or ductile. Thus it can be seen that the electrodes with dissimilar diameters lead to full plug failure which is failure occurring in the surrounding material while the welds remain intact under the applied mechanical loading, which explains that this mode of welds have been able to transmit a high level of force, thus leading to severe plastic deformation in adjacent components. While in the case of weld obtained with similar diameters of used electrodes it is clear that the interfacial failure occurred at the nugget of the weld, and according according Pouranvari et al[10], such failure mode can be considered as brittle and less energy absorbing than plug failures in addition the Load carrying capacity and energy absorption capability for those welds that fail under interfacial mode are much less than those which fail under plug failure mode.

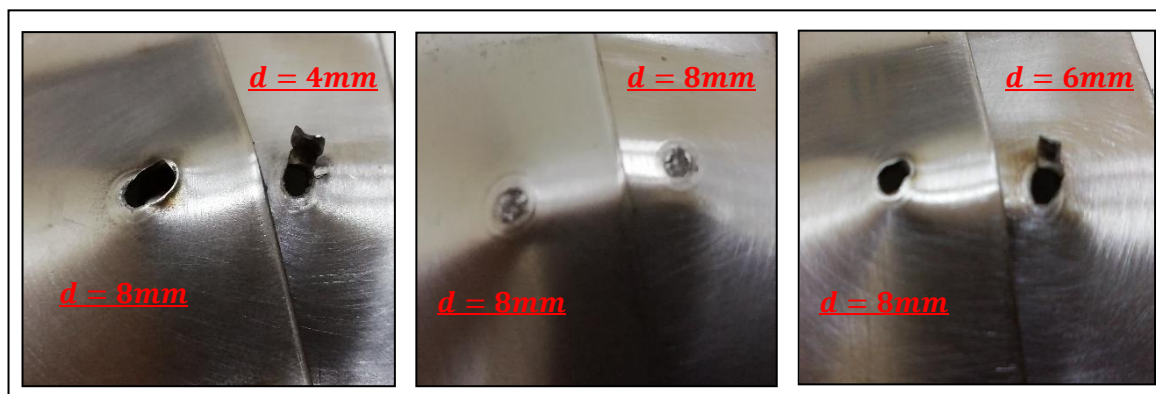


Figure 7: Images of test specimen with different failure modes resulted from the cross-tensile tests of the performed welds

3.4 Shear tensile behavior

Overlap shear tensile testing provides data on the ultimate strength of the resistance spot welded joint and the failure mode. Compared to cross tensile tests the results are less dependent on the exact location of the weld. Indeed, shear tensile properties resulted from the shear tensile tests of all samples are shown in Fig.8.

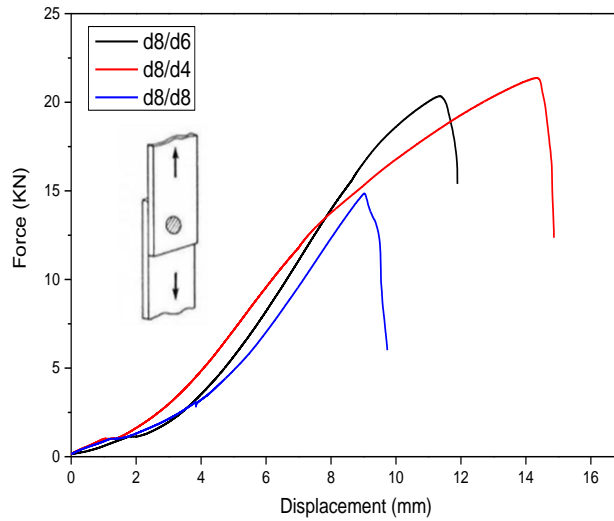


Figure 8: Shear-tensile curves of welds obtained with: d8/d8, d8/d6 and d8/d4

It can be seen from Fig.8 that the higher shear tensile strength is found in the case of the sample welded using electrodes with dissimilar diameters d8/d4, while the lower shear strength is observed in the specimen welded using electrodes with similar diameters d8/d8. On the other hand, the analysis of failure mode after the shear loading is presented in Fig.9. It can be seen that the common failure mode of all samples is the so-called interfacial fracture, the nugget is divided into two sections due to the applied shear loading. Moreover, from these fractured welds, one may remark that there is a clear correlation between the diameter of electrodes used for welding and the resulted nugget size. Consequently, the sample welded using electrodes with similar diameters (d8/d8) exhibited a smaller nugget size while the higher is found in the case of dissimilar diameters (d8/d4). Therefore the nugget size is behind the mechanical properties difference.

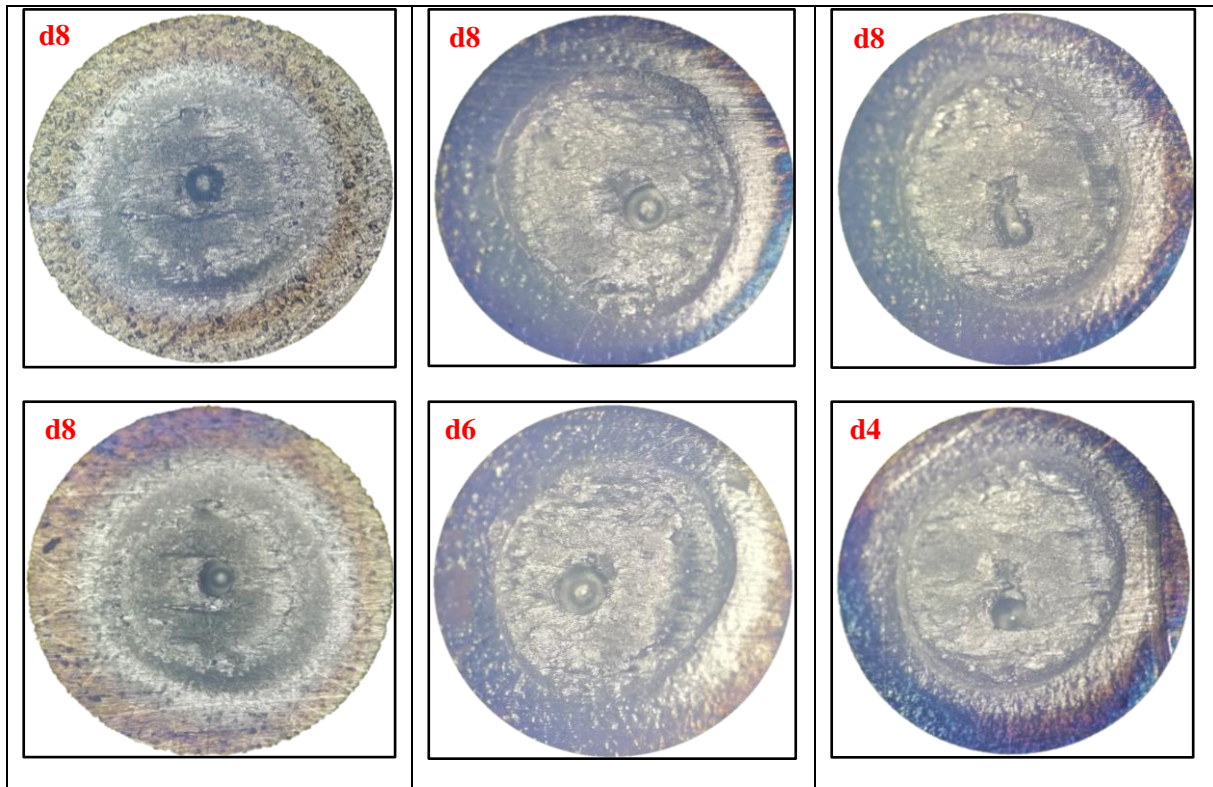


Figure 9: Images of test specimen with different failure modes resulted from the shear-tensile tests of the performed welds

IV. CONCLUSION

Resistance spot welding (RSW) of the investigated steel using electrodes with similar and dissimilar diameters was carried out in this study, based on the microstructural and mechanical results, the following conclusions can be drawn:

- Using electrodes with dissimilar diameters, leads to a decrease in the contact area from side between the electrodes and the sheet metal. As the area decreases, the current density increases. An increase in current density leads to an increase in heat generation. Thus the nugget size increases and while its shape becomes non uniform;
- welds load bearing capacities depends strongly on the electrodes diameter, an increase of welds was found when using dissimilar electrodes for welding;

s

ACKNOWLEDGEMENT

The authors are grateful to the "Metallurgy Laboratory of High National School of Arts and Crafts ENSAM- Meknès- Morocco " .

REFERENCES

- [1] T. R. Mahmood, Q. M. Doos, and A. M. Al-Mukhtar, "Failure Mechanisms and Modeling of Spot Welded Joints in Low Carbon Mild Sheets Steel and High Strength Low Alloy Steel," in *Procedia Structural Integrity*, 2018, vol. 9, pp. 71–85, doi: 10.1016/j.prostr.2018.06.013.
- [2] M. I. Khan, M. L. Kuntz, E. Biro, and Y. Zhou, "Microstructure and Mechanical Properties of Resistance Spot Welded Advanced High Strength Steels," *Mater. Trans.*, vol. 49, no. 7, pp. 1629–1637, Jul. 2008, doi: 10.2320/matertrans.MRA2008031.
- [3] N. J. den Uijl, "Laser Weld Induced Microstructural Changes in Automotive Bodysheet," *Math. Model. weld Phenom.* 7.
- [4] H. Essoussi, S. Elmouhri, S. Ettaqi, and E. Essadiqi, "Microstructure and mechanical performance of resistance spot welding of AISI 304 stainless steel and AISI 1000 series steel," in *Procedia Manufacturing*, 2019, vol. 32, pp. 872–876, doi: 10.1016/j.promfg.2019.02.296.
- [5] M. Kahn, *Spot welding of advanced high strength steels*. 2007.
- [6] R. Rana and S. B. Singh, *Automotive Steels: Design, Metallurgy, Processing and Applications*. 2016.
- [7] K. R. Chan, N. Scotchmer, J. C. Bohr, I. Khan, M. L. Kuntz, and Y. N. Zhou, "EFFECT OF ELECTRODE GEOMETRY ON RESISTANCE SPOT WELDING OF AHSS."
- [8] P. Ravichandran, C. Anbu, B. Meenakshipriya, and S. Sathiyavathi, "Process parameter optimization and performance comparison of AISI 430 and AISI 1018 in resistance spot welding process," *Mater. Today Proc.*, Jun. 2020, doi: 10.1016/j.matpr.2020.05.197.
- [9] M. Vinosh, T. Nithish Raj, and M. Prasath, "Optimization of sheet metal resistance spot welding process fixture design," *Mater. Today Proc.*, Oct. 2020, doi: 10.1016/j.matpr.2020.08.567.
- [10] M. Pouranvari and S. P. H. Marashi, "Critical review of automotive steels spot welding: Process, structure and properties," *Science and Technology of Welding and Joining*, vol. 18, no. 5. Taylor & Francis, pp. 361–403, Jul-2013, doi: 10.1179/1362171813Y.0000000120.